AGRONOMY (AGRONOMIA)

Spectral analysis of soils in the lower course of the Acaraú River, Northeastern Brazil

Rafael Cipriano da Silva[1], Gustavo Souza Valladares[2], Marcos Gervasio Pereira[3]*

[1] Fundação Cearense de Meteorologia e Recursos Hídricos, Fortaleza, CE, Brasil. E-mail: ciprorafael@gmail.com
[2] Universidade Federal do Piauí, Teresina, PI, Brasil. E-mail: valladares@ufpi.edu.br
[3] Universidade Federal Rural do Rio de Janeiro, Seropédica, RJ, Brasil. E-mail: mgervasiopereira01@gmail.com

ABSTRACT: The objective of this research was to analyze the spectral response of alluvial soils, representative of the coastal plain in the lower course of the Acaraú River, Ceará, Brazil, and to correlate with the granulometry and soil organic matter (SOM) contents, seeking to identify the best method to predict the attributes studied. In four soil profiles (n = 23 soil samples) the sand, silt, and clay and SOM contents were determined and was carried out the mineralogical characterization. Soil samples were submitted to spectral analysis using a spectroradiometer, with spectral range from visible to shortwave to near infrared (350 - 2,500 nm). It was possible to relate the soil attributes such as color, SOM contents, variation in granulometry and even mineralogy aspects, such as types of minerals in the clay fraction, with the spectral reflectance curves. Some spectral interpretations were useful in understanding aspects associated with the genesis of these soils, especially with regard to the formation environment and mineralogy. For the SOM contents, the best estimates were obtained by simple linear regression and higher correlation for the 564 nm spectrum range. Regression methods were efficient in estimating soil attributes, but the study is limited to the small sample size.

Key words: pedometry; sedimentary soils; semi-arid soils; spectral curves

Análise espectral de solos do Baixo Curso do Rio Acaraú, nordeste do Brasil

RESUMO: Objetivou-se com esta pesquisa analisar a resposta espectral de solos aluviais, representativos de planície litorânea no Baixo Curso do Rio Acaraú, Ceará, Brasil, e correlacionar com a granulometria e teores de matéria orgânica do solo (MOS), buscando identificar o melhor método para predizer os atributos estudados. Em quatro perfis de solo (n = 23 amostras de solo) foram determinados os teores de areia, silte e argila, os teores de MOS e realizada a caracterização mineralógica. As amostras de solo foram submetidas à análise espectral com uso de um espectrorradiômetro, com faixa espectral de visível para ondas curtas ao infravermelho próximo (350 - 2.500 nm). Foi possível relacionar os atributos do solo como cor, teores de MOS, variação na granulometria e até aspectos mineralogia, como tipos de minerais da fração argila, com as curvas de refletância espectral. Algumas interpretações espectrais foram úteis na compreensão de aspectos associados à gênese desses solos, principalmente no que diz respeito ao ambiente de formação e mineralogia. Para os teores de MOS, as melhores estimativas foram obtidas por regressão linear simples e maior correlação para a faixa do espectro de 564 nm. Os métodos de regressão foram eficientes na estimativa de atributos de solos, mas o estudo limita-se ao pequeno número amostral.

Palavras-chave: pedometria; solos sedimentares; solos do semiárido; curvas espectrais

Introduction

Soil is an indispensable resource for a series of activities fundamental to the maintenance of human life, such as the production of food, fiber, and energy, the provision of environmental services, the sustaining of biodiversity, and the maintenance of water sources (TCU, 2015). Soil survey and mapping study in Brazil is necessary precisely to underpin the planning of these activities associated with land use and conservation. However, these studies are still deficient given the large extension of the national territory and the financial and technical limitations (Carvalho Junior et al., 2017).

For this reason, the Tribunal de Contas da União (TCU), through its operational audit on governance of non-urban soils (TCU, 2015), pointed out that insufficient knowledge about Brazilian soils compromises the planning, execution, and monitoring of public policies for sustainable land use. As a result, the TCU recommended the Ministério da Agricultura, Pecuária e Abastecimento (MAPA) and the Empresa Brasileira de Pesquisa Agropecuária (Embrapa) to establish collaborative and permanent mechanisms for the organization, systematization and operation of data from soil surveys. This action aims to contribute to the development of new mappings and in guiding the use of new tools and the evolution of mapping methods.

In this context, pedometrics has much to contribute because it deals with the application of mathematical and statistical methods for the study of soil distribution, thus assisting in the creation of methodologies for soil evaluation and mapping (Minasny et al., 2014; Carvalho Junior et al., 2017). Soil analysis procedures using proximal sensors, such as spectroradiometers, streamline and decrease mapping costs (Carvalho Junior et al., 2017). Spectral characterization of soils in the visible (VIS: 350-780 nm) and near infrared (NIR: 780-2,500 nm) ranges stands out as it is a fast, simple and low-cost method (Demattê et al., 2019; Ribeiro et al., 2021).

Spectral characterization of soils is an efficient method that makes it possible to correlate spectral results with pedogenesis, assisting in soil surveys (Minasny et al., 2014; Terra et al., 2018; Poppiel et al., 2019) and in evaluating areas through satellite imagery (Demattê et al., 2016). Currently, the most studied spectral characterization of soils is in the visible (VIS: 350-780 nm) and near infrared (NIR: 780-2,500 nm) bands, which allows correlating with properties such as grain size, soil organic matter (SOM) contents, exchangeable cations, and mineralogy (Pinheiro et al., 2017; Poppiel et al., 2019; Coblinski et al., 2020; Ribeiro et al., 2021).

In the State of Ceará, Brazil, although the exploratory soil map on the scale of 1:600,000 (Jacomine et al., 1973) is still adopted as reference, a new soil mapping on the scale of 1:100,000 is being carried out, missing about 12% of the total area of the territory, which corresponds to the part of the west coast of the State. In this region is located the Irrigated Perimeter of Baixo Acaraú, which covers the municipalities of Acaraú, Bela Cruz and Marco and stands out for its socioeconomic importance, being considered the second largest of the irrigable area of the federal irrigated perimeters (Nascimento et al., 2006). However, the region suffers from environmental problems, resulting mainly from the indiscriminate use of the soil and the absence of efficient public policies, compromising the productive capacity of the soils and causing degradation. However, in the region, not many pedological studies are observed characterizing the great variation and heterogeneity of soil attributes recurrent to the pedogenetic conditions influenced by the fluvial dynamics of the Acaraú River, with emphasis on the high sand contents and restricted areas with organic matter accumulation (Nascimento et al., 2006).

Coupled with this, there is still the fact that the spectral characterization of soils in the semi-arid region, especially those of alluvial origin, is still lacking information. And in the semi-arid coastal strip of Brazil this information becomes even more scarce. Thus, the spectral characterization of soils collected in the lower course of the Acaraú River, Ceará, Brazil, can contribute to the correlation with soil attributes such as SOM content, granulometry and mineralogy, thus aiming to obtain a better knowledge of the soils of the region. The objective of this research was to analyze the spectral response of representative soils of the coastal plain in the Western region of Ceará, Brazil, and correlate it to the granulometry and SOM attributes. In addition, we sought to identify the best method to predict the attributes studied.

Materials and Methods

Characterization of the study area

The study was carried out in the lower course of the Acaraú River, Northern region of Ceará State, Brazil (Figure 1). The region climate is type As, according to the Köppen classification, with the rainy season concentrated between the months of January and May, and the dry season in the spring (September to December). The average annual temperature is 25 °C, average air humidity is 70%, average annual precipitation is 1,030 mm, and evapotranspiration is 1,600 mm (Diniz et al., 2008; Andrade et al., 2018).

The geological substratum of the region is mainly composed of metamorphic rocks of the crystalline basement (Precambrian), such as granites, migmatites, gneisses, schists, quartzites and phyllites (Falcão Sobrinho, 2006). This substrate is covered by alluvial and eolic sediments of the Barreiras Group and Serra Grande Formation (Falcão Sobrinho, 2006). River plains and fluvial terraces occur in the region (with 0 to 3% slope), formed by clay and silty sediments, while near the coast there is a predominance of marine plains influenced by the tidal regime and covered by sandy sediments (Falcão Sobrinho, 2006; Diniz et al., 2008).

For this study four areas whose soils are considered representative for the lower course of the Acaraú River region were selected, chosen based on preliminary studies and field observations that identified, along the river plains, soils such as Luvisols (Luvissols), Leptosols (Neossolos Litólicos), Cambisols (Cambissolos), and Fluvisols
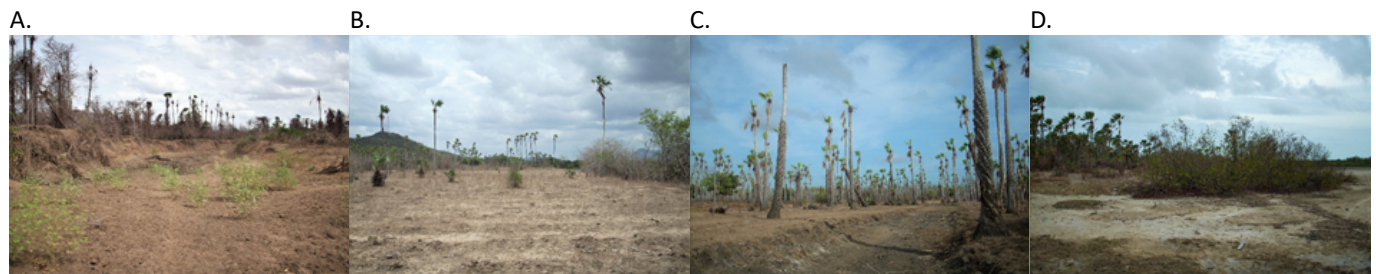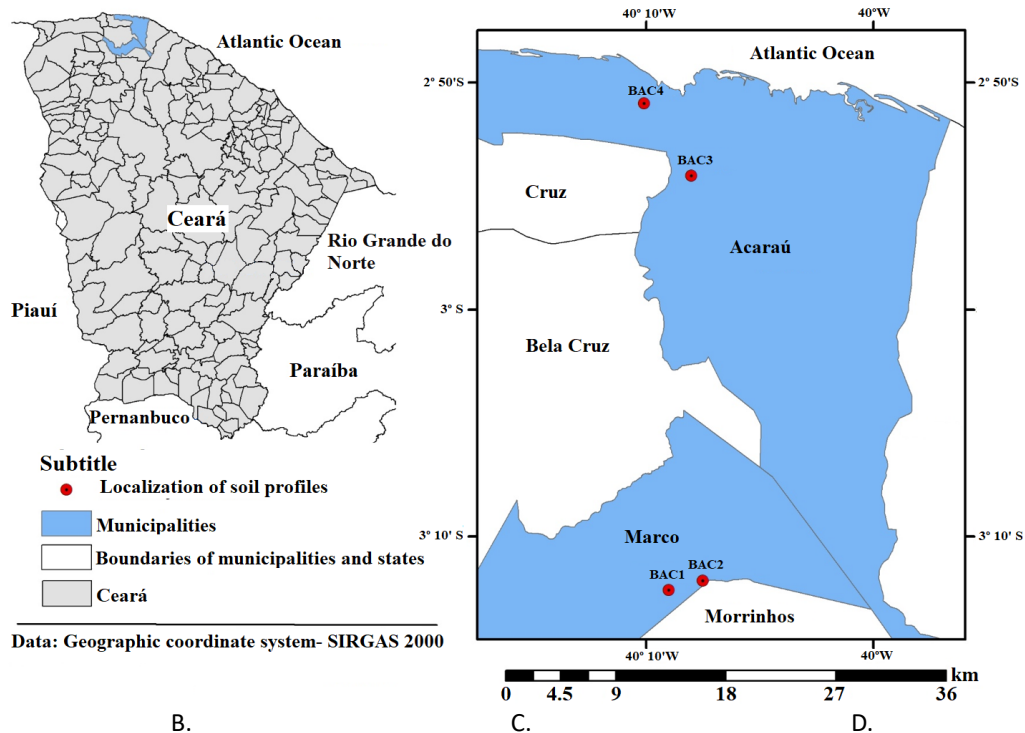
Figure 1. Schematic of location and situation of soil profiles in the State of Ceará for the municipalities of Acaraú and Marco (Zone 24; UTM coordinates). Points on the map and photographs indicate the environments of the collection points of the profiles: BAC1 (A), BAC2 (B), BAC3 (C), and BAC4 (D).

(Neossolos Flúvicos), sometimes associated with Planosols (Planossolos), besides Gleysols (Gleissolos) and Arenosols (Neossolos Quartzarênicos) that become frequent as the river approaches the coast (Jacomine et al., 1973; Nascimento et al., 2006; Santos et al., 2018). In each selected area a soil profile was opened, morphological descriptions and sampling were performed according to Santos et al. (2015). One sample per horizon was collected, totaling 23 soil samples, which were later air dried, crushed and passed through a stainless steel sieve with a 2 mm mesh to obtain the air dried fine soil (ADFS). Soil profiles were classified according to the World Reference Base for Soil Resources (IUSS Working Group WRB, 2015) and the Brazilian Soil Classification System (SiBCS) (Santos et al., 2018).

Methods and analysis

In this study, particle size analysis was performed, using the pipette method, with the use of 0.1 mol L^{-1} sodium hexametaphosphate as a dispersing agent (Teixeira et al., 2017). The determination of total organic carbon (TOC) contents was performed by the wet oxidation method, using potassium dichromate, and subsequent conversion of TOC contents into SOM using the conversion factor (f) of 1.724 (Teixeira et al., 2017).

For the qualitative analysis of soil mineralogy only one horizon per profile was chosen. A Miniflex II X-ray diffractometer (XRD) (Rigaku, Tokyo) with CuKα radiation (30kV and 15 mA) and Ni filter was used. Clay samples were treated to remove Fe oxides with dithionite-citrate-bicarbonate (DCB) solution and then saturated with potassium and irradiated at 25, 350, and 550 °C; they were also saturated with Mg and solvated with ethylene glycol at 60 °C. The clay samples were mounted on oriented slides. The sand fraction of the soil was separated by sieving, milled in agate mortar, and the powdered sheets were assembled. The samples were irradiated at a step of 0.02° 2θ s^{-1}, in the range from 3° to 50° 2θ.

For the spectral analysis, all soil samples were previously dried at 45 °C, sieved with a mesh diameter ≤ 2 mm and then homogeneously distributed in Petri dishes. A Fieldspec 3 spectroradiometer (Analytical Spectral Devices - ASD, Boulder, CO) was used, with a spectral range from visible to shortwave to near infrared (350 - 2,500 nm) and spectral resolution of 1 nm from 350 to 700 nm, 3 nm from 700 to 1,400 nm, and 10 nm from 1,400 to 2,500 nm. The sampling interval of the data output is 1 nm, reporting 2,151 channels.

The spectral sensor, which was used to capture the light via a fiber optic cable, was allocated 8 cm from the sample surface. The sensor scanned an area of approximately 2 cm^2 and a light source was provided by two 50 W external halogen lamps. These lamps were positioned at a distance of 35 cm from the sample (uncollimated rays and a zenith angle of 30°) with a 90° angle between them. A Spectralon standard white plate was scanned every 20 minutes during calibration. Two repetitions (one involving a 180° turn of the Petri dish) were obtained for each sample. Each spectrum was calculated from 100 readings over 10 seconds. The average values from two repetitions were used for each sample.

The results of the soil analyses were explored using descriptive statistics (minimum, mean, maximum, standard deviation, skewness, and kurtosis). The spectral data were treated qualitatively and then simple linear correlation and partial correlation analyses were performed between the attributes of the soils studied and the spectral results obtained. The soil attributes were tested by the Kolmogorov-Smirnov test and, due to the lack of fit with the normal distribution, the SOM contents were transformed, according to Equation 1, and the granulometric attributes, according to Equation 2.

$$SOMt = \log(SOM + 1) \tag{1}$$

$$Xt = \log(X) \tag{2}$$

where:

SOMt - transformed SOM value by the logarithmic function; and,

Xt - transformed value by the logarithmic function of the variables clay, sand or silt content.

The highest modulus value electromagnetic spectrum bands were analyzed to determine the linear correlation with each soil attribute. Simple and multiple linear regression analyses were also performed using the stepwise method, applied to the reflectance data of the studied range associated with the analytical variables of each soil attribute (SOM and clay, silt and sand contents). The data were also treated by partial least squares regression (PLSR). Measures such as the coefficient of determination (R^2), the simple linear correlation coefficient (r), the average absolute error (ABE), the root mean square error (RMSE), and the residual prediction deviation (RPD) were calculated in order to evaluate the performance of the estimates for each attribute evaluated.

Results and Discussion

General characterization of soil profile attributes

Among the studied profiles, BAC1 and BAC2 have imperfect drainage, while BAC3 and BAC4 are poorly drained presenting (Table 1). In the latter two, morphological characteristics associated with the hydromorphic condition were verified with greater expression, such as neutral colors and the presence of mottling and variegated coloration (Table 2) (Santos et al., 2015). The morphological description of the profiles, as well as the sand, silt, clay and SOM contents are described in Table 2.

The SOM contents range from 0.9 to 12.9 g kg^{-1}, with an average of 6.5 g kg^{-1} and show a slight asymmetry and very high frequency in the central class of the histogram, whose contents range from 5.5 to 8.3 g kg^{-1} (Figure 2A). The SOM contents range from 0.9 to 12.9 g kg^{-1}, with an average of 6.5 g kg^{-1} and show a slight asymmetry and very high frequency in the central class of the histogram, whose contents range from 5.5 to 8.3 g kg^{-1} (Figure 2A). Evaluating the spectral response of Neossolos Flúvicos in the Chapada do Apodi, CE, Brazil, Ribeiro et al. (2021), also found high heterogeneity of soil carbon contents. Of the 23 soil samples, only in two soil samples are SOM contents higher than 10 g kg^{-1} (equivalent to 6 g kg^{-1} TOC) identified. These two samples correspond to two superficial horizons from profiles BAC3 (Apnz horizon) and BAC4 (Agnz horizon), both hydromorphic. Unusually in the case of these two profiles, the higher SOM contents is a result of the reduced environment by water saturation (Cipriano-Silva et al., 2020), decreasing microbial activity and SOM decomposition.

Table 1. General information and classification of soil profiles collected in lower course of the Acaraú River, Ceará, Brazil.

Profiles	Vegetation and use	Drainage	Source material	Classification[1] WRB	Classification[1] SiBCS
BAC1	Hypoxerophilic Caatinga with presence of 'carnaúbas' (*Copernicia prunifera*)	Imperfectly drained	Sediments of alluvial origin	Eutric Sodic Fluvisol (Loamic)	Neossolo Flúvico Sódico sálico
BAC2	Hypoxerophilic Caatinga with the presence of 'carnaúba' (*Copernicia prunifera*) associated with natural pastures	Imperfectly drained	Sediments of alluvial origin	Eutric Fluvic Planosol (Loamic)	Planossolo Háplico Eutrófico solódico
BAC3	'Carnaúbas' (*Copernicia prunifera*) associated with natural pastures	Poorly drained	Sediments of alluvial origin	Sodic Vertisol (Hypereutric)	Vertissolo Hidromórfico Sódico salino
BAC4	Saline fields with halophyte plants	Poorly drained	Sediments of alluvial origin	Fluvic Sodic Gleyic Solonchak (Hypersalic, Loamic)	Gleissolo Sálico Sódico típico

[1] WRB - World Reference Base for Soil Resources (IUSS Working Group WRB, 2015); SiBCS - Brazilian Soil Classification System (Santos et al., 2018).

Table 2. Morphological description (color), grain size fractionation (sand, silt, and clay), total organic carbon content (TOC), and mineralogy of sand and clay fractions in four profiles located in lower course of the Acaraú River, Ceará, Brazil.

Horizons	Depth (cm)	Color (humid)[1]	Sand	Silt	Clay	SOM	Mineralogy [2]	
			(g kg⁻¹)				Sand	Clay
BAC1								

Table 2. Morphological description (color), grain size fractionation (sand, silt, and clay), total organic carbon content (TOC), and mineralogy of sand and clay fractions in four profiles located in lower course of the Acaraú River, Ceará, Brazil.

Horizons	Depth (cm)	Color (humid)[1]	Sand	Silt	Clay	SOM	Mineralogy [2] Sand	Mineralogy [2] Clay
			(g kg⁻¹)					
BAC1- Eutric Sodic Fluvisol (Loamic) - (Neossolo Flúvico)								
A	0-16	10YR 4/3 **	622	199	179	7.2		
CA	16-38	10YR 3/3	320	328	353	7.2		
Cnz1	38-92	10YR 4/2	372	291	337	6.4		
Cnz2	92-132	10YR 4/2	359	343	298	4.5		
2Cnz	132-155	2.5YR 4/2 **	494	275	231	2.8		
3Cvn	155-175+	10YR 4/1 *	321	395	285	4.3	quartz (abd), feldspars (cm)	kaolinite (abd), esmectita + illita (cm)
BAC2- Eutric Fluvic Planosol (Loamic) – (Planossolo)								
A	0-20	10YR 3/4	649	214	138	8.6		
2A	20-33	10YR 4/4	389	237	375	5.7		
2E	33-50	10YR 5/3	904	43	54	1.4		
2EB	50-60	10YR 5/4 **	693	183	125	2.4		
2Bt1	60-71	Var. 10YR 5/3 and 10YR 3/3	144	548	309	8.1		
2Bt2	71-98	Var. 10YR 5/3 and 10YR 4/3	210	514	277	6.4		
2Btvnz	98-140+	10YR 4/3	151	463	387	8.3	quartz (abd), feldspars (cm)	kaolinite (abd), esmectita + illita (cm)
BAC3- Sodic Vertisol (Hypereutric) - (Vertissolo)								
Apnz	0-25	10YR 2/3	172	295	534	12.9		
CA	25-47	10YR 3/3	155	315	531	8.6		
Cvn	47-80	10YR 5/2	250	312	439	5.7	quartz (abd), feldspars (cm)	kaolinite (abd), esmectita + illita (cm)
2Cn	80-120+	Var. 2.5Y 6/2 and 7.5YR 6/8	977	3	20	0.9		
BAC4- Fluvic Sodic Gleyic Solonchak (Hypersalic, Loamic) - (Gleissolo)								
Agnz	0-8	Var. 5YR 4/4 and 5YR 3/4	798	122	80	11.7		
Cgnz1	8-32	2.5Y 5/2 **	634	194	173	5.2		
Cgnz2	32-50	5Y 4/1 ***	521	215	265	7.4	quartz (abd).	kaolinite (abd), esmectita + illita (cm)
2Cgnz	50-72	N4/ *	226	480	295	8.3		
3Cgnz	72-80	N4/ *	716	134	151	6.6		
4Cgnz	80-110+	N2/	836	94	70	8.8		
Minimum			143	3	20	0.9		
Average			474	269	257	6.5		
Maximum			977	548	534	12.9		
Standard deviation			264	146	144	3		
Asymmetry			0.33	0.17	0.2	0.01		
Kurtosis			-1.3	-0.8	-0.9	-0.34		

[1] Presence of mottling in quantity: * low; ** common; *** abundant. [2] Relative amount, determined based on X-ray diffractometry (XRD), of minerals in the soil: abundant (abd), common (cm).

The proportion of the granulometric fractions is variable, both among profiles and among horizons within the same profile, with medium texture predominating in BAC1, BAC2 and BAC4, while clayey texture predominates in BAC3 (Table 2). The presence of soils with a more clayey texture in BAC3, compared to BAC2 and BAC1 is associated with low fluvial energy that favors the selection of finer grained materials, while in BAC4 it is governed by marine influence.

The sand contents are asymmetric and bimodal distribution, with the highest frequency observed between 100 and 270 g kg⁻¹ (Figure 2B). Silt contents are also asymmetric and bimodal distribution (Figure 2C), with the highest frequency occurring in the 110 to 330 g kg⁻¹. The lack of normal distribution in the grain size fractions is due to the erratic distribution of the grain size of sediments deposited by the action of rivers, a common characteristic in soils with fluvial character (Santos et al., 2018; Cipriano-Silva et al., 2020).

Among the particle size fractions, clay is the closest to the normal distribution (unimodal) (Figure 2D), with the highest frequency near the mean value, between 215 and 320 g kg⁻¹; however, with high frequency at the extremities. This clay fraction pattern may be related to the nature of the parent material that presents greater homogeneity in the particle size composition of the alluvial sediments, which is influenced by the relationship between the carrying capacity of the water runoff and the force required to displace the solid particles
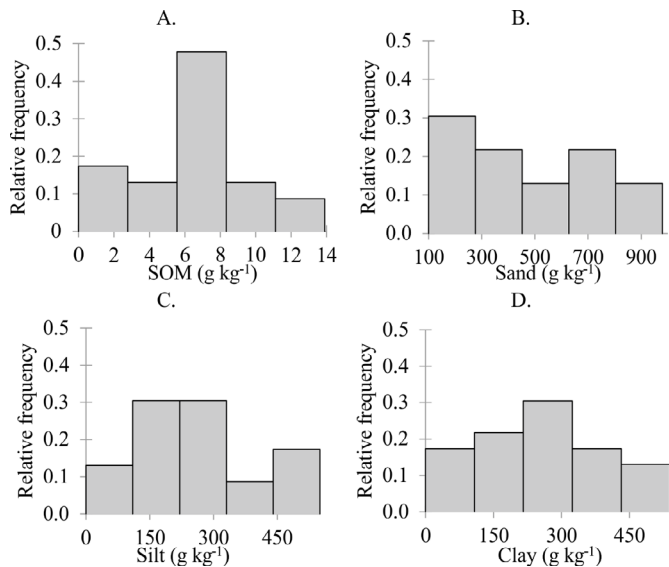
Figure 2. Histograms with frequency distribution of soil organic matter (SOM) content and sand, silt, and clay content of soil samples from four profiles located in the lower course of the Acaraú River, Ceará, Brazil.

along the river course. The normal distribution for particle size attributes was observed by Coblinski et al. (2020), in a study carried out in Rio Grande do Sul, Southern region of Brazil, in which 66 collection points were evaluated at three depths in an area of soils formed from igneous rocks and alluvial deposits, and whose texture varied from very clayey to sandy.

Spectral curves of the soil samples

The reflectance intensity of the spectral curves, absorption bands, and the features of the curves can be interpreted by visual analysis (Coblinski et al., 2020). Variations in reflection curves and intensity are observed both between profiles and between horizons within the same profile (Figure 3). Among the attributes, soil grain size and SOM content have a strong influence on the shapes of spectral curves in the VIS-NIR range (Demattê et al., 2016; Viscarra Rossel et al., 2016; Pinheiro et al., 2017; Romero et al., 2018; Coblinski et al., 2020).

The two samples with higher sand contents, corresponding to horizons 2Cn of Vertisol (Figure 3C) and 2E of Planosol (Figure 3B), present higher reflection intensity of the electromagnetic spectrum, with values in the range of 1,700 to 1,850 nm higher than 0.6, showing that the sandy texture increases the reflection intensity at this wavelength. In the range between 500 and 1,300 nm, these curves have a different pattern from the other horizons of soil profiles, a typical characteristic of sandy-textured soils (Tian & Philpot, 2015).

Generally, higher SOM contents are observed in the surface horizons, resulting in spectral curves with lower reflection intensity in the range between 400 and 1,200 nm (Demattê et al., 2016; Viscarra Rossel et al., 2016; Pinheiro et al., 2017; Ribeiro et al., 2021). However, this reflection pattern is not observed in the VIS range of the profiles (Figure 3A, 3B, and 3D), the presence of the erratic distribution of C at depth, gives the Fluvisol, Planosol and Solonchak profiles the fluvial character (Table 2).
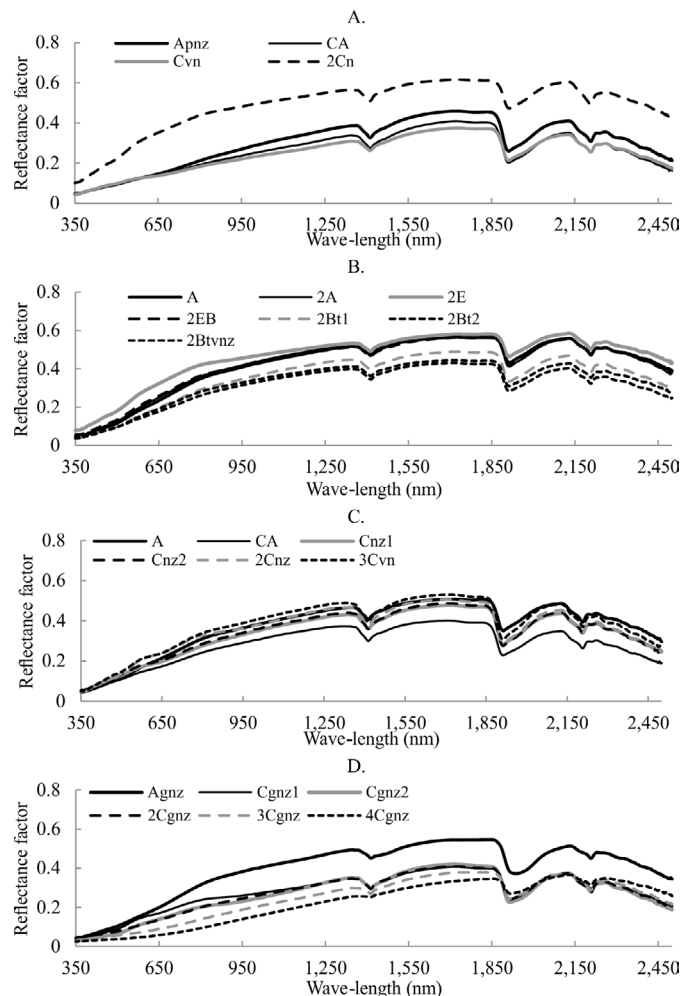

Figure 3. Spectral curves of the horizons of four profiles located in the lower course of the Acaraú River, Ceará, Brazil. (A) Sodic Eutric Fluvisol (loamic), (B) Fluvic Eutric Planosol (loamic), (C) Sodic Vertisol (Hypereutric), and (D) Gleyic Sodic Solonchak (hypersalic, loamic).

The A horizon of Solonchak (Figure 3D) shows a high reflection intensity compared to the other horizons in the profile. This pattern is related to salinity, since high values of electrical conductivity are verified in Solonchak, attributing it a salic character, i.e., < 7 dS m^{-1} (subscript z; Santos et al., 2018) (Table 2), according to a characterization study conducted by Cipriano-Silva et al. (2020) in this same profile. The wavelengths between 1,900 and 1,480 nm have high relationship with salts such as NaCl and MgCl, thus related to salinity of soils (Aldabaa et al., 2015). Thus, higher salinity increases the reflectance indices at this wavelength (Wang et al., 2018), due to the formation of saline efflorescences on the aggregate and soil surface and which exhibit light color.

The pattern of the spectral curves of the medium-textured and clayey horizons of Vertisol, Planosol, Fluvisol and the shallower C horizons of Solonchak are very similar, both in intensity and shape. No absorption bands of iron oxides (goethite and hematite) are observed between 450 and 530 nm or in the range 700 to 900 nm, indicating little concentration of these minerals in these soils, due to impeded or imperfect

Rev. Bras. Cienc. Agrar., Recife, v.17, n.2, e2258, 2022

6/11

drainage. Absorption bands of argillominerals are observed at 1,400, 1,900, and 2,200 nm, with highest absorption in the band near 1,900 nm, indicating predominance of 2:1 clays (Poppiel et al., 2019), such as smectites and illite, identified in the horizons by XRD (Table 2). The asymmetry in the band at 2,200 nm also indicates the presence of 1:1 kaolinite mineral (Demattê et al., 2017; Coblinski et al., 2020; Ribeiro et al., 2021). These results are consistent with the results of the mineralogy of the clay fraction (Table 2) and demonstrate the ability of spectroscopy to identify features associated with soil clay minerals, since in many cases the use of XRD is hampered, both by lack of equipment and by the delay in sample preparation.

For the last two C horizons of the Solonchak profile a distinct pattern from the other studied profiles is seen, in the range between 350 and 1,850 nm, with a very pronounced, concave-shaped absorption. In these horizons neutral colors are verified (N 4/ and N 2/; Table 2), with the latter, darker in color, showing less reflection, this pattern can be attributed as a function of the SOM present in the soils (Pinheiro et al., 2017).

Analysis of the correlations between the studied attributes and the spectral response

The SOM shows positive, weak and significant correlation at 5.2% probability with clay content (r = 0.41) and negative, weak and significant correlation with sand content at 7.2% probability (r = -0.38). The sand contents show strong negative correlation with the clay and silt contents (both r = 0.91). For clay content there is a positive and significant correlation at 0.1% (r = 0.65) with silt. Soils with a more clayey texture tend to have higher SOM and silt contents compared to those with a sandier texture, indicating collinearity between the attributes. In addition to the input of organic material by vegetation and anaerobic conditions (oxidation and reduction), it is important to note that soil texture also influences SOM contents, since the clay fraction is an important component for SOM occlusion (Schweizer et al., 2019). Thus, the sandier the texture, the faster the SOM decomposition tends to be.

Figure 4 show the linear correlations between the attributes SOM, clay, sand and silt, respectively, and the reflectance index between 350 and 2,500 nm. As for SOM, the band of the electromagnetic spectrum near 570 nm has the highest inversely proportional correlations. In the entire spectrum range the r values are negative, indicating that higher SOM contents reduce the reflectance indices (Pinheiro et al., 2017). This pattern is due to the dark colors of the humic compounds present in the SOM, conditioning low albedo up to 1,350 nm, that is, they increase the absorption of electromagnetic energy in this range of the spectrum. Between 350 and 968 nm is the range of the spectrum where the correlation coefficients are most significant, with p < 0.01 (Figure 4A). By visual interpretation, the bands of the spectrum where the greatest weakening of the correlation with SOM occurs are at 1,400, 1,900, and 2,200 nm, which correspond to spectra associated with the presence of the
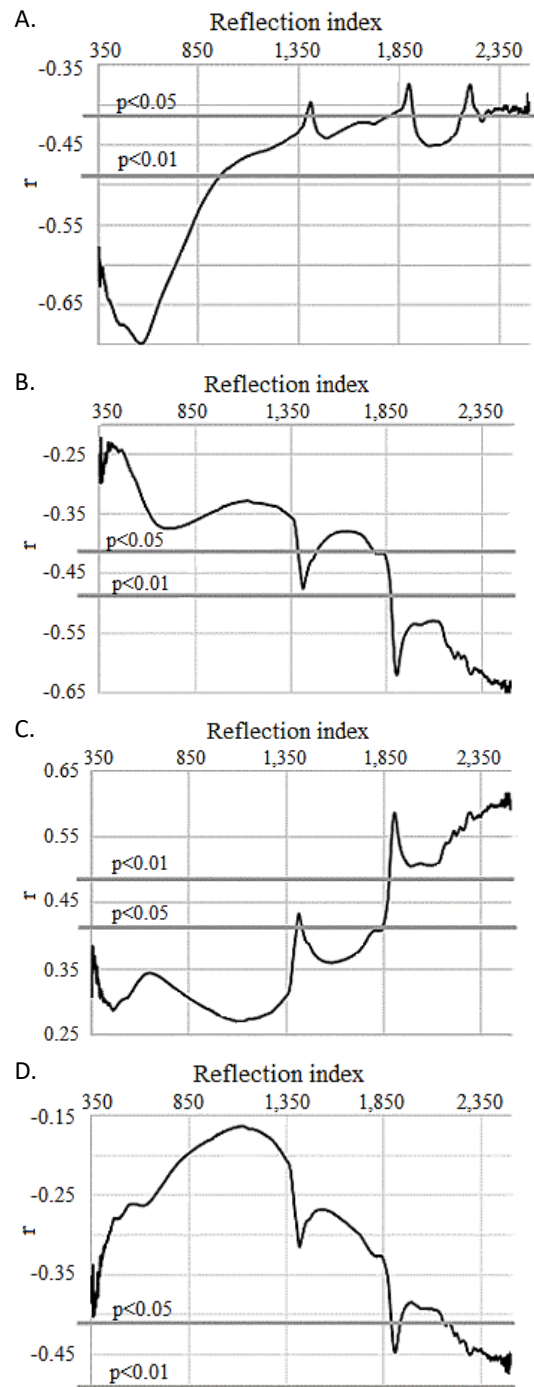

Figure 4. Reflectance index for SOM, clay, sand and silt contents of soil samples from four profiles located in the lower course of the Acaraú River, Ceará, Brazil. Gray lines indicate the simple linear correlation coefficients at 5% and 1% probability (p = 0.05 and 0.01; respectively). (A) soil organic matter, (B) clay, (C) sand, and (D) silt.

1:1 and 2:1 silicate clays and also the presence of water and hydroxyls from the crystalline structures of the clays (Coblinski et al., 2020).

Clay content shows a negative correlation with reflectance indices, as does SOM. However, the correlation is strongest and most significant in the spectrum range between 1,874 and 2,500 nm (Figure 4B), in contrast to what is observed

Rev. Bras. Cienc. Agrar., Recife, v.17, n.2, e2258, 2022

7/11

for SOM where in VIS-NIR it is strongest. Higher correlation occurs at 1,400 nm, but mainly at 1,900 nm, indicating the presence of 2:1 clays, and between 2,200 and 2,500 nm, with 2,200 nm being the range of occurrence of 1:1 clays (Coblinski et al., 2020).

For sand contents, the opposite pattern is seen to those for SOM and clay, indicating that more sandy soils have higher reflectance rates, especially in the range from 1,877 to 2,500 nm (Tian & Philpot, 2015), where the r values are significant at p < 0.01 (Figure 4C). In the longer wavelength range, near 2,500 nm, the correlations are the strongest. The silt contents show the negative and lower correlation coefficients compared to the clay, sand and SOM contents, being significant at 5% probability only in the range 1,900 nm and between 2,200 and 2,500 nm (Figure 4D).

To investigate the spectrum bands representing the silicate clays (1,400, 1,900, and 2,200 nm) partial correlations of the soil attributes and the reflectance indices in these bands were established (Table 3). With the partial correlation analysis it is possible to see that the clay fraction has the greatest influence on the reflectance indices in these bands. The results indicate that the collinearity of clay contents with those of sand, silt, and SOM generates false correlation of these attributes with the reflectance indices of the studied soils. It is found that there is no correlation for sand in the 1,400, 1,900, and 2,200 nm ranges, which makes sense, since the sand fraction of soils, consisting predominantly of quartz, has no water or OH$^-$ bonds in its crystalline structure. When the effect of the sand and clay fractions is taken into account, the partial correlation coefficient values are close to zero. According to Coblinski et al. (2020), quartz has its pattern best explained in the spectrum bands above 2,500 nm.

A similar pattern to sand is verified for silt (Table 3), highlighting that this fraction is also composed predominantly of quartz. Evaluating the correlation of the silt contents in the VIS band at 358 nm, where a peak occurs, it is possible to observe weak but significant partial correlation of the silt in this band of the spectrum, with the false correlation being that of the clay and sand in this band.

For SOM there is a higher simple linear correlation in the spectrum at 570 nm, (Figure 4A). With the aid of the partial correlation (Table 3), the greatest effect is observed in this 570 nm range, obtaining a coefficient value of 0.70. Next to the clay fraction, this partial correlation coefficient is -0.66, both significant at 1% probability. However, the analysis shows no correlation of clay when evaluating the effect of SOM at 570 nm (Table 3).

Estimation of soil attribute contents by different regression methods

The validation of the methods used to estimate the soil attributes is presented in Table 4, with the best models from the validation measures. However, compared to other studies, such as those by Pinheiro et al. (2017) and Coblinski et al. (2020), whose prediction models were generated from a high sample number (over 100 samples), the models generated in this study are limited in terms of the low sample number. Ribeiro et al. (2021), conducting studies with two sample groups, totaling 65 soil samples, were successful in estimating TOC content using hyperspectral remote sensing.

For the SOM contents, the simplest methods, that is, the less labor-intensive and complex, were the ones that presented the best estimates, in this case those of simple linear regression. This analysis shows that the spectrum band 564 nm shows the highest correlation with the investigated attribute, and the best fit is the one in which the SOM was transformed by a logarithmic function with base 10. Since some SOM values were between 0 and 1 the sum of the constant 1 was used, so that there would be no negative data after the transformation.

To calculate the validation measures, the inverse of the logarithmic function was used where the estimated data were transformed from SOMt to SOM. Therefore, this method had the highest values for coefficient of determination (R^2) and RPD, and the lowest for ABE and RMSE. For SOM, the RPD value is 1.46, which is considered satisfactory and can show good estimates. The R^2 is high, at 0.86, indicating that in the validation set 86% of the data is explained by the model. The ABE is only 0.01, demonstrating that the mean of the residuals approached zero, which occurs with perfect models, which is not the case here.

Table 3. Simple and partial linear correlation coefficients and reflectance indices determined for SOM, clay, silt, and sand contents of soil samples from profiles located in the lower course of the Acaraú River, Ceará, Brazil.

Variable	Electromagnetic spectrum bands (nm)				
Variable.Covariable	358	570	1,400	1,900	2,200
SOM	-	-0.70****	-0.40**	-0.37**	-0.38**
SOM.Clay	-	-0.66****	-0.27	-0.17	-0.19
Clay	-0.29*	-0.32*	-0.45***	-0.62****	-0.59****
Clay.SOM	-0.05	-0.05	-0.34*	-0.55****	-0.51****
Clay.Silt	-0.05	-	-	-	-
Sand	0.38**	-	0.40**	0.58****	0.55****
Sand.Clay	-	-	-0.01	0.07	0.06
Sand.Silt	0.05	-	-	-	-
Silt	-0.40**	-	-	-0.44***	-0.42***
Silt.Clay	-0.29*	-	-	-0.07	-0.06

**** - p < 0.01; *** - p < 0.05; ** - p < 0.10; * -p < 0.15.

Table 4. Results of the validation of the best fit model determined for SOM, clay, sand and silt contents of soil samples from profiles located in the lower course of the Acaraú River, Ceará, Brazil.

Attribute	Prediction model	Equation	ABE	RMSE	RPD	R²
SOM	SLR 1	Log SOM = 1.25 − 2.655 × c564	0.01	2.43	1.46	0.86
Clay	MLR 2	Clay content = 392.93 + 1,882.96 × c1415 − 2,937.60 × c2490	-30.56	102.69	1.41	0.74
Sand	SLR 3	Total sand = − 120.61 + 2,024.99 × c2488	95.78	177.95	1.23	0.54
Silt	PLSR	-	-74.82	102.26	0.86	0.38

Where: c564, c2490, and c2488 are, respectively, reflection ratios at wavelengths 564, 2,490, and 2,488 nm; SOM: soil organic matter; SLR: simple linear regression; MLR: multiple linear regression; PLSR: partial least squares regression.

The linear regression with the original SOM data shows RPD of 1.35, with R^2 of 0.86, RMSE of 2.63 and ABE of -0.46, indicating that the method underestimates the data. However, according to Chang et al. (2001), RPD values less than 1.4 are not reliable. The PLSR method, efficient in research with soils from the Amazon (Pinheiro et al., 2017) and other regions of the world (Viscarra Rossel et al., 2016), shows estimation considered weak with RPD less than 1.4, for original SOM and with transformed data (SOMt), with results with SOMt being slightly higher. For the non-linear and multiple regressions no good results are seen.

The values for the clay, sand and silt fractions were transformed because, similarly to what was observed for the SOM, no normal distribution was found for these fractions. Multiple regression was the model that resulted in the best estimates for clay contents, selecting two independent variables, the wavelengths of 1,415 and 2,490 nm. The RPD is 1.41, a satisfactory value for estimating the variables (Chang et al., 2001), and the R^2 coefficient is 0.74. All other methods obtained RPD less than 1.4, with the second best fit being the simple linear regression method using the 2,490 nm band. Transformation of the clay content data does not result in better estimates and validation of the methods.

For sand contents, good results are verified for the simple linear regression as a function of the 2,488 nm band, with R^2 of 0.54, but with RPD of 1.23, a value that indicates a model of moderate quality for estimates. Since it is less than 1.40 the quality of this estimate tends to be worse for sand compared to clay and SOM (Chang et al., 2001). For this model the fit occurred with the original sand data, without the logarithmic transformation. The studies of Pinheiro et al. (2017), conducted with 434 soil samples from the Central Amazon region; and Coblinski et al. (2020), in an evaluation of 197 soil samples from the Southern region of Brazil, both aimed at relating spectral curves with soil granulometry, also verified a better fit for clay when compared to sand, a possible explanation for this pattern is the better response of this attribute in wavelengths above 2,500 nm.

The silt contents do not show satisfactory fits, with a RPD value of less than 1, which means very poor quality estimates. Simple linear regression with untransformed data is not significant. The model that shows the best fit is PLSR with the original silt values, with R^2 of 0.38 and RPD of only 0.86, both very low and with very poor prediction. Other studies also found worse prediction for silt compared to clay and sand and associated the worse estimation for silt due to the original

method determining this fraction by difference (Viscarra Rossel et al., 2016; Pinheiro et al., 2017; Coblinski et al., 2020).

Conclusions

Through the spectral characterization of alluvial soils, formed in lowland environments, it was possible to identify features associated with attributes such as color, soil organic matter content, and relationship with sand, silt, and clay content. It was also possible to relate the spectral behavior of the soils to aspects associated with their genesis, such as hydromorphic condition, the presence of salts in Solonchack, and the presence of 2:1 and 1:1 clay minerals.

The regression methods were efficient in estimating attributes of alluvial soils of the lower course of the Acaraú River, Ceará, Brazil, which present great variation in SOM contents and granulometry. The spectral indices of the different bands of the electromagnetic spectrum in the VIS-NIR range show correlation with SOM and grain size. For the SOM contents the best fitting models were identified, followed by the clay and sand contents. The silt contents had unsatisfactory fits. The low sample size can influence the reliability of the model results.

Acknowledgments

Compliance with Ethical Standards

Author contributions: Conceptualization: GSV, MGP; Data curation: RCS; Formal analysis: RCS; Funding acquisition: GSV; Investigation: RCS; Methodology: RCS, GSV; Resources: GSV; Supervision: GSV, MGP; Visualization: RCS, GSV, MGP; Writing – original draft: RCS; Writing – review & editing: GSV, MGP.

Conflict of interest: The authors declare that there are no possible conflicts of interest (professional or financial) that could influence the article.

Literature Cited

Aldabaa, A.A.A.; Weindorf, D.C.; Chakraborty, S.; Sharma, A.; Li, B. Combination of proximal and remote sensing methods for rapid soil salinity quantification. Geoderma, v.239-240, p.34-46, 2015. https://doi.org/10.1016/j.geoderma.2014.09.011.

Andrade, G.R.P.; Cuadros, J.; Partiti, C.S.M.; Cohen, R.; Vidal-Torrado, P. Sequential mineral transformation from kaolinite to Fe-illite in two Brazilian mangrove soils. Geoderma, v.309, p.84-99, 2018. https://doi.org/10.1016/j.geoderma.2017.08.042.

Carvalho Júnior, W.; Santos, M.L.M.; Anjos, L.H.C. Contribuições da pedometria para a governança de solos e o Pronasolos. Boletim Informativo da Sociedade Brasileira de Ciência do Solo, v. 43, n. 3, p. 38-41, 2017. https://ainfo.cnptia.embrapa.br/digital/bitstream/item/170796/1/2017-093.pdf. 19 Jan. 2022.

Chang, C.W.; Laird, D.A.; Mausbach, M.J.; Hurburgh, C.R. Near-infrared reflectance spectroscopy–principal components regression analyses of soil properties. Soil Science Society of America Journal, v.65, n.2, p.480, 2001. https://doi.org/10.2136/sssaj2001.652480x.

Cipriano-Silva, R.; Valladares, G.S.; Azevedo, A.C.; Anjos L.H.C.; Pereira, M.G.; Pinheiro Junior C.R. Alluvial soil formation in the plains of northeastern Brazil. Revista Brasileira de Ciência do Solo, v.44, e0190110, 2020. https://doi.org/10.36783/18069657rbcs20190110.

Coblinski, J.A.; Giasson, É.; Demattê, J.A.; Dotto, A.C.; Costa, J.J.F.; Vašát, R. Prediction of soil texture classes through different wavelength regions of reflectance spectroscopy at various soil depths. Catena, v.189, e104485, 2020. https://doi.org/10.1016/j.catena.2020.104485.

Demattê, J.A.M; Carnieletto Dotto, A.; Paiva, A.F.S.; Sato, M.V.; Dalmolin, R.S.D.; Araújo, M. do S.B. de; Silva E. B. da; Nanni, M.R.; ten Caten, A.; Noronha, N.C.; Lacerda, M.P.C.; Araújo Filho, J.C. de; Rizzo, R.; Bellinaso, H.; Francelino, M.R.; Schaefer, C.E.G.R.; Vicente, L.E.; Santos, U.J. dos; Sampaio, E.V.de S.B.; Menezes, R.S.C.; Souza, J.J.L.L.de; Abrahão, W.A.P.; Coelho, R.M.; Grego, C.R.; Lani, J.L.; Fernandes, A.R.; Gonçalves, D.A.M.; Silva, S.H.G.; Menezes, M.D. de; Curi, N.; Couto, E.G.; Anjos, L.H.C. dos; Ceddia, M.B.; Pinheiro, É.F.M.; Grunwald, S.; Vasques, G.M.; Marques Júnior, J.; Silva, A.J. da; Barreto, M.C. de V.; Nóbrega, G.N.; Silva, M.Z. da; Souza, S.F. de; Valladares, G.S.; Viana, J.H.M.; Terra, F. da S.; Horák-Terra, I.; Fiorio, P.R.; Silva, R.C. da; Frade Júnior, E.F.; Lima, R.H.C.; Alba, J.M.F.; Souza Junior, V.S. de; Brefin, M. de L.M.S.; Ruivo, M. de L.P.; Ferreira, T.O.; Brait, M.A.; Caetano, N.R.; Bringhenti, I.; Mendes, W. de S.; Safanelli, J.L.; Guimarães, C.C.B.; Poppiel, R.R.; Souza, A.B. e; Quesada, C.A.; Couto, H.T. Z. do. The Brazilian soil spectral library (BSSL): a general view, application, and challenges. Geoderma, v.354, e113793, 2019. https://doi.org/10.1016/j.geoderma.2019.05.043.

Demattê, J.A.M.; Alves, M.R.; Terra, F.S.; Bosquilia, R.W.D.; Fongaro, C.T.; Barros, P.P.S. Is it possible to classify topsoil texture using a sensor located 800 km away from the surface? Revista Brasileira de Ciência do Solo, v.40, e0150335, 2016. https://doi.org/10.1590/18069657rbcs20150335.

Demattê, J.A.M.; Horák-Terra, I.; Beirigo, R.M.; Terra, F.S.; Marques, K.P.P.; Fongaro, C.T.; Silva, A.C.; Vidal-Torrado, P. Genesis and properties of wetland soils by VIS-NIR-SWIR as a technique for environmental monitoring. Journal of Environmental Management, v.197, p.50–62, 2017. https://doi.org/10.1016/j.jenvman.2017.03.014.

Diniz, S.F.; Moreira, C.A.; Corradini, F.A. Susceptibilidade erosiva do baixo curso do rio Acaraú-CE. Geociências, v.27, n.3, p.355-367, 2008. https://www.periodicos.rc.biblioteca.unesp.br/index.php/geociencias/article/view/3413/2858. 10 Jan. 2022.

Falcão Sobrinho, J. A compartimentação geomorfológica do Vale do Acaraú: distribuição das águas e pequeno agricultor. Mercator, v. 10, v. 5, p. 91-110, 2006. http://www.mercator.ufc.br/mercator/article/view/70/45. 17 Feb. 2022.

IUSS Working Group WRB. World reference base for soil resources 2014, update 2015. International soil classification system for naming soils and creating legends for soil maps. Rome: FAO, 2015. 192 p. (World Soil Resources Reports, 106). https://www.fao.org/3/i3794en/I3794en.pdf. 19 Jan. 2022.

Jacomine, P.K.T.; Almeida, J.C.; Medeiros, L.A.R. Levantamento exploratório - reconhecimento de solos do Estado do Ceará. Recife: Sudene-DRN; Brasília: Divisão de Pesquisa Pedológica, 1973. 2v. (Brasil. Divisão de Pesquisa Pedológica. Boletim técnico, 28; Sudene-DRN. Série Pedologia, 16).

Minasny, B.; Malone, B.; Stockmann, U.; Odgers, N.; McBratney, A.B. Pedometrics. Reference Module in Earth Systems and Environmental Sciences, 2014. https://doi.org/10.1016/b978-0-12-409548-9.09163-6.

Nascimento, F.R.; Cunha, S.B.; Rosa, M.F. Classes de solos e unidades morfo-pedológicas na bacia hidrográfica do Rio Acaraú, Ceará. In: Simpósio Nacional de Geomorfologia/Regional Reference on Geomorphology, 6., 2006, Goiânia. Anais... Goiânia: International Association of Geomorphologists; Brazilian Geormorphological Union, 2006. http://lsie.unb.br/ugb/sinageo/6/1/016.pdf. 19 Jan. 2022.

Pinheiro, E.F.; Ceddia, M.B.; Clingensmith, C.M.; Grunwald, S.; Vasques, G.M. Prediction of soil physical and chemical properties by visible and near-infrared diffuse reflectance spectroscopy in the central Amazon. Remote Sensing, v. 9, n.4, e293, 2017. https://doi.org/10.3390/rs9040293.

Poppiel, R.R., Lacerda, M.P., Demattê, J.A., Oliveira Júnior, M.P., Gallo, B.C., Safanelli, J.L. Pedology and soil class mapping from proximal and remote sensed data. Geoderma, v. 348, p. 189-206, 2019. https://doi.org/10.1016/j.geoderma.2019.04.028.

Ribeiro, S.G.; Teixeira, A.D.S.; Oliveira, M.R.R.; Costa, M.C.G.; Araújo, I.C.D.S.; Moreira, L.C.J.; Lopes, F. B. Soil organic carbon content prediction using soil-reflected spectra: a comparison of two regression methods. Remote Sensing, v. 13, n. 23, e4752, 2021. https://doi.org/10.3390/rs13234752.

Romero, D.J.; Ben-Dor, E.; Dematte, J.A.M.; Souza, A.B.E.; Vicente, L.E.; Tavares, T.R.; Martello, M.; Strabeli, T.F.; Barros, P.P. da S.; Fiorio, P.R.; Gallo, B.C.; Sato, M.V.; Eitelwein, M.. Internal soil standard method for the Brazilian soil spectral library: performance and proximate analysis. Geoderma, v. 312, p. 95-103, 2018. https://doi.org/10.1016/j.geoderma.2017.09.014.

Rev. Bras. Cienc. Agrar., Recife, v.17, n.2, e2258, 2022

10/11

Santos, H.G.; Jacomine, P.K.T.; Anjos, L.H.C.; Oliveira, V.A.; Oliveira, J.B.; Coelho, M.R.; Lumbreras, J.F.; Cunha, T.J.F. Sistema brasileiro de classificação de solos. 5.ed. Rio de Janeiro: Embrapa Solos, 2018. 353p. http://www.infoteca.cnptia.embrapa.br/infoteca/handle/doc/1094003. 19 Jan. 2022.

Santos, R.D.; Lemos, R.C.; Santos, H.G.; Ker, J.C.; Anjos, L.H.C. Manual de descrição e coleta de solo no campo. 7.ed. Viçosa: Sociedade Brasileira de Ciência do Solo, 2015. 101p.

Schweizer, S.A.; Bucka, F.B.; Graf-Rosenfellner, M.; Kögel-Knabner, I. Soil microaggregate size composition and organic matter distribution as affected by clay content. Geoderma, v. 355, e113901, 2019. https://doi.org/10.1016/j.geoderma.2019.113901.

TCU - Tribunal de Contas da União. Auditoria operacional em governança de solos não urbanos. Brasília: TCU, 2015. https://portal.tcu.gov.br/biblioteca-digital/auditoria-operacional-em-governanca-de-solos-nao-urbanos.htm. 01 Feb. 2022.

Teixeira, P.C.; Donagemma, G.K.; Fontana, A.; Teixeira, W.G. Manual de métodos de análise de solo. 3.ed. Brasília: Embrapa, 2017. 574p. http://www.infoteca.cnptia.embrapa.br/infoteca/handle/doc/1085209. 01 Feb. 2022.

Terra, F.S.; Demattê, J.A.M.; Viscarra Rossel, R.A. Proximal spectral sensing in pedological assessments: Vis–NIR spectra for soil classification based on weathering and pedogenesis. Geoderma, v.318, p.123-136, 2018. https://doi.org/10.1016/j.geoderma.2017.10.053.

Tian, J.; Philpot, W.D. Relationship between surface soil water content, evaporation rate, and water absorption band depths in SWIR reflectance spectra. Remote Sensing of Environment, v. 169, p. 280–289, 2015. https://doi.org/10.1016/j.rse.2015.08.007.

Viscarra Rossel, R.A.; Behrens, B.D.; Brown, D.J.; Demattê, J.A.M.; Shep-Herd, K.D.; Shi, Z.; Stenberg, B.; Stevens, A.; Adamchuk, V.; Aïchi, H.; Barthès, B.G.; Bartholomeus, H.M.; Bayer, A.D.; Bernoux, M.; Böttcher, K.; Brodský, L.; Du, C.W.; Chappell, A.; Fouad, Y.; Genot, V.; Gomez, C.; Grunwald, S.; Gubler, A.; Guerrero, C.; Hedley, C.B.; Knadel, M.; Morrás, H.J.M.; Nocita, M.; Ramirez-Lopez, L.; Roudier, P.; Rufasto Campos, E.M.; Sanborn, P.; Sellitto, V.M.; Sudduth, K.A.; Rawlins, B.G.; Walter, C.; Winowiecki, L.A.; Hong, S.Y.; Ji, W. A global spectral library to characterize the world's soil. Earth-Science Reviews, v. 155, p. 198–230, 2016. https://doi.org/10.1016/j.earscirev.2016.01.012.

Wang, J.; Ding, J.; Abulimiti, A.; Cai, L. Quantitative estimation of soil salinity by means of different modeling methods and visible-near infrared (VIS–NIR) spectroscopy, Ebinur Lake Wetland, Northwest China. PeerJ, v. 6, e4703, 2018. https://doi.org/10.7717/peerj.4703.